PREDICTION OF CUTTING FORCE IN END MILLING OF INCONEL 718

M.S. Kasim[1,*], C.H. Che Haron[2], J.A. Ghani[2], N. Mohamad[1], R. Izamshah[1], M. Minhat[1], S.B. Mohamed[3], J.B Saedon[4], N.H Saad[4]

[1]Faculty of Manufacturing Engineering, Universiti Teknikal Malaysia Melaka, 76100 Hang Tuah Jaya, Melaka.

[2]Faculty of Engineering and Built Environment, Universiti Kebangsaan Malaysia, 43600 Bangi, Selangor.

[3]Faculty of Design and Engineering Technology, Universiti Sultan Zainal Abidin, Gong Badak 21300 Kuala Terengganu, Terengganu.

[4]Faculty of Mechanical Engineering, Universiti Teknologi MARA, 40450 Shah Alam, Selangor.

ABSTRACT

This paper presents the effect of cutting parameters on the cutting force when machining Inconel 718. Response surface methodology (RSM) was used in the experiment, and a Box–Behnken design was employed to identify the cause and effect of the relationship between the four cutting parameters (cutting speed, feed rate, depth of cut and width of cut) and cutting force. The ball-nose type of end mill with donwmill approach was maitained througout the experiment. The forces were measured using Kistler dynamometer during straight line machining strategy. The result shows that the radial depth of cut was the dominating factor controlling cutting force, it was followed by axial depth of cut and feed rate. The prediction cutting force model was developed with the average error between the predicted and actual cutting force was less than 3%.

KEYWORDS: Inconel 718; end mill; cutting force; response surface method; perturbation plot; high-speed machining

1.0   INTRODUCTION

Inconel is well-known to be one of the hardest materials to be machined. Due to its stability during extreme temperature, it is widely used for applications requiring high temperature strength resistance (Kitagawa, et al., Ulutan & Ozel, 2011). As an example, more than five hundred

---

* Corresponding author email: shahir@utem.edu.my

jet turbine engine element are fabricated using Inconel 718 (Kalluri & Halford, 1995). However, one of its limitation is poor machinability, which is due to high strength property and abrasive particle, causing short tool life (Sharman, et al., 2001). These problems are related to materials deformation and friction at vicinity region of tool-chip and tool-workpiece interface (Ezugwu, et al., 1999; Izamshah, et al., 2012). During machining of this material, the temperature rise leads to an increase in material's toughness and thus increase in cutting force (Liao, et al., 2008). Studies by Ezugwu et al., (2005). Kitagawa et al., (1997). found that the cutter suffered in notch wear near DOC line during machining of Inconel 718. It was indicated that the notch wear started with pitting and chipping on cutting edge due to interrupted cutting process. Kasim et al., (2013) found that the maximum force exerted onto rake face in the moment after tool engagement with the workpiece. The failure modes of flaking on a rake face and notch wear on the flank face are associated with the combination of cyclic load and maximum force on the depth of cut (DOC) line. The result of these failures causes the cutting tool to fail catastrophically.

Design of experiment (DOE) is a systematic method to determine the relationship between uncontrollable inputs affecting the controlled output of the process (Montgomery, 2009). This statistical tool is widely used to replace time consuming trial and error basis. DOE helps to simplify to experimental process. A large number of studies have been conducted to determine the optimal machining process. As an example, Saedon et al., (2014) attempted a study on multi objectives optimization on WEDM of Ti6Al4V. The error between prediction and experimental of surface roughness was 2%. Amran et al., (2013) reported on surface roughness on drilling process. Based on their study in drilling process, the surface roughness was decreased as the spindle speed, feed rate and tool diameter increased. A mathematical model of surface finish during turning of Ti6Al4VELi was developed by Sulaiman et al., (2014). In their study, a statistical model was developed using RSM as to predict the cutting force during the milling process and identify the minimum cutting force. Here, it was observed that the occurrence of notch wear can be delayed and usable life of the cutting tool can be prolonged.

2.0   METHODOLOGY

The work material used was a rectangular block of aged Inconel 718 (AMS 5663 grade) with the yield strength and hardness of 1034 MPa and 44 HRc respectively (Alloys, 2011). The chemical composition of the workpiece material is shown in Table 1.

Table 1. Inconel 718 compositions.

Al	B	C	Cb.Ta	Co	Cr	Cu	Fe	Mn	Mo
0.49	0.004	0.051	5.05	0.30	18.30	0.04	18.70	0.23	3.05
Ni	P	S	Si	Ti					
53.0	< 0.005	< 0.002	0.08	1.05					

The insert was coated with TiAlN/AlCrN multilayer PVD coating with WC-10% Co; 10 Ø mm; radial rake angle 0°; axial rake angle -3° and relief angle 11°. The milling operations were carried out on the DMC 635 V Eco CNC milling machine with a maximum speed of 8000 RPM. The cutting forces were measured using a Kistler model 5070 A dynamometer. The cutting parameters are cutting speed, feed rate, depth and width of cut. Accordance to Box-Behnken technique, the number of trials is 29 for four factors including 5 center points. The cutting force was recorded throughout single-pass cutter with the fresh cutting condition. The cutting parameter for this study is shown in Table 2.

Table 2. Experimental level of the independent variables and coding.

Factor\Level	-1	0	1
Cutting speed, V_c (m/min)	100	120	140
Feed rate, f_z (mm/tooth)	0.1	0.15	0.2
Depth of cut, a_p (mm)	0.5	0.75	1.0
Width of cut, a_e (mm)	0.2	1	1.8

3.0   RESULT AND DISCUSSION

The measured cutting forces (Fx, Fy, Fz) are plotted in Figure 1a. For ball nose end milling, Fx is found to be dominating cutting force of 64%, followed by Fy (19%) and Fz (17%) as shown in Figure 1b.
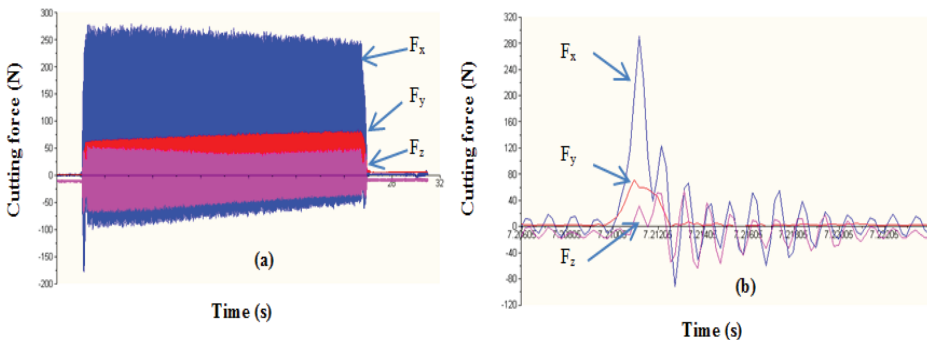

Figure 1. Component of cutting force during end milling.

The resultant force, F_r , consisting of three major cutting-force component, F_x, F_y, F_z associated with the force direction of x, y, z axis respectively. This parameter is calculated by employing an expression as given in Equation (1) Alauddin, et al., (1996), with the results as listed in Table 3.

$$F_r = \sqrt{F_x + F_y + F_z} \tag{1}$$

From the experimental results, it is apparent that ball nose end milling can achieve low cutting force which initiated from 157 N up to a maximum of 466 N. Similar findings were reported by previous work on milling of Inconel 718 Alauddin, et al., (1998a, 1998b, 1998c, 1998d).

Table 3. Cutting force results of different cutting conditions.

No.	V_c (m/min)	fz (mm/tooth)	ap (mm)	ae (mm)	F_X (N)	F_Y (N)	F_Z (N)	Resultant Force, F_t (N)
1	100	0.15	0.75	0.2	185.50	54.23	57.13	201.53
2	120	0.15	1	0.2	238.91	78.80	72.66	261.85
3	120	0.1	1	1	293.03	89.95	65.95	313.54
4	120	0.15	0.75	1	301.47	85.53	75.68	322.38
5	100	0.15	0.75	1.8	321.00	105.51	63.14	343.75
6	120	0.15	0.5	0.2	141.11	54.34	44.07	157.50
7	140	0.15	0.75	0.2	170.36	54.66	61.07	189.05
8	120	0.2	0.5	1	274.75	69.96	85.85	296.23
9	120	0.2	0.75	0.2	208.79	64.33	86.36	234.92
10	120	0.15	0.75	1	309.37	92.00	75.68	331.52
11	120	0.1	0.75	0.2	158.63	52.02	52.86	175.11
12	120	0.1	0.5	1	195.97	68.02	53.07	214.12
13	140	0.15	0.75	1.8	345.70	103.79	72.54	368.17
14	120	0.15	0.75	1	288.07	73.85	70.80	305.70
15	120	0.1	0.75	1.8	247.74	73.29	60.85	265.42
16	120	0.2	0.75	1.8	416.58	122.45	98.69	445.28
17	100	0.2	0.75	1	351.53	83.47	93.66	373.25
18	140	0.15	0.5	1	243.97	74.20	58.14	261.55
19	120	0.15	0.5	1.8	250.78	82.31	47.61	268.20
20	120	0.15	1	1.8	418.40	105.99	96.80	442.33
21	100	0.15	0.5	1	233.17	67.03	61.62	250.32
22	140	0.15	1	1	376.68	103.55	78.77	398.51
23	100	0.1	0.75	1	229.22	71.40	59.11	247.25
24	140	0.1	0.75	1	222.21	67.60	60.09	239.91
25	120	0.2	1	1	440.26	98.21	115.78	465.70
26	100	0.15	1	1	358.93	82.99	94.06	380.22
27	140	0.2	0.75	1	367.34	119.81	71.08	392.87
28	120	0.15	0.75	1	290.21	76.05	83.77	311.48
29	120	0.15	0.75	1	281.04	66.88	83.68	300.76

The analysis of variance (ANOVA) was applied to check the adequacy of the model and determine the significance of effects. From ANOVA analysis, as given in Table 4, the F-Value of 245.52 indicates that the model is significant. This is supported by the lack of fit value of 0.63, which implies that the model is not significant. The Box-Behnken quadratic model shows that width of cut, *ae*, has the highest effect on cutting force, followed by axial depth of cut, *ap*, and feed rate, *fz*. It was also observed that the cutting speed, V_c is not significant on the exerted force. Therefore, this non-significant cutting parameter was removed from the model. This reduction of V_c term does not affect the prediction model since the coefficient in model is too small which can be neglected. Furthermore, there is very marginal difference between R^2 (0.987) and the adjusted R^2 (0.984). These observations suggested that this model can be applied due to the lack of fit probability model is 77.7%. Hence, the probability to be poor discrepancy between observed values and the values expected of the statistical model is very low.

Table 4. ANOVA for the second order model of cutting force.

Source	Sum of squares	DF	Mean square	F- Value	Prob > F	
Model	188469.7	7	26924.25	245.52	< 0.0001	Significant
fz	47238.58	1	47238.58	430.76	< 0.0001	
ap	55248.76	1	55248.76	503.80	< 0.0001	
ae	69490.95	1	69490.95	633.67	< 0.0001	
ae²	10444.39	1	10444.39	95.24	< 0.0001	
fz.ap	1226.974	1	1226.974	11.12	0.0031	
fz.ae	3602.47	1	3602.47	32.85	< 0.0001	
ap.ae	1217.633	1	1217.633	11.10	0.0032	
Residual	2302.932	21	109.6634			
Lack of fit	1676.142	17	98.59661	0.63	0.7774	Not significant
Pure error	626.7894	4	156.70			
Cor total	190772.7	28				

2.1   Statistical equation model for resultant force

From the experimental results, a statistical equation model was developed to estimate the resultant force through all significant factors using normal model transformation. The resultant force, F_r, can be predicted by the following second-order model which shown in Equation (2):

where f_z is feed rate, ap axial depth of cut and ae is width of cut. The comparison has been made between actual and calculated value as shown in Figure 2, the average error for 29 trials being approximately 2.6%.
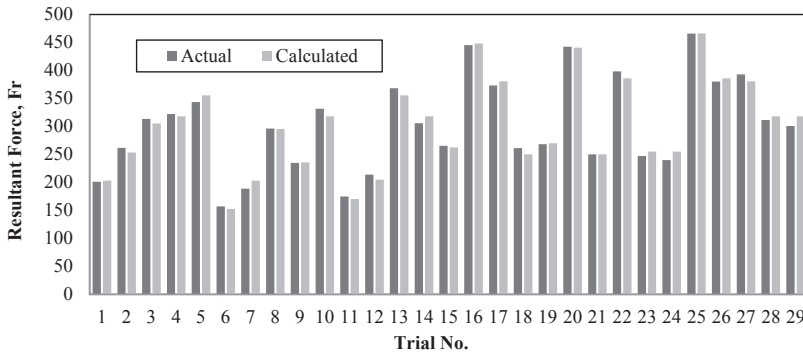
$$F_r = 106.43 - 546.26\ fz - 26\ ap + 37.6\ ae - 60.2\ ae^2 + 1401.13\ fz.ap + 750.26\ fz\ .ae + 87.24\ ap.ae \qquad (2)$$

where f_z is feed rate, *ap* axial depth of cut and *ae* is width of cut. The comparison has been made between actual and calculated value as shown in Figure 2, the average error for 29 trials being approximately 2.6%.

Figure 2. Experiment and calculation comparison with average error of 2.6%.

The optimum cutting parameters to obtain the lowest resultant force of 150.23 N were Vc = 125.7 m/min, fz = 0.12 mm/tooth, ap = 0.52 mm and ae = 0.22 mm. It is clearly presented in a perturbation plot in Figure 3 that the optimum value is achieved at the negative ends of every factor studied in this work. It shows positive response in reducing the resultant force which normally reduces the tool life in machining process. Besides, it is an interesting point to be noted that factor C and D would further decrease the optimum value for the minimum resultant force by shifting the factors to the lower ranges.
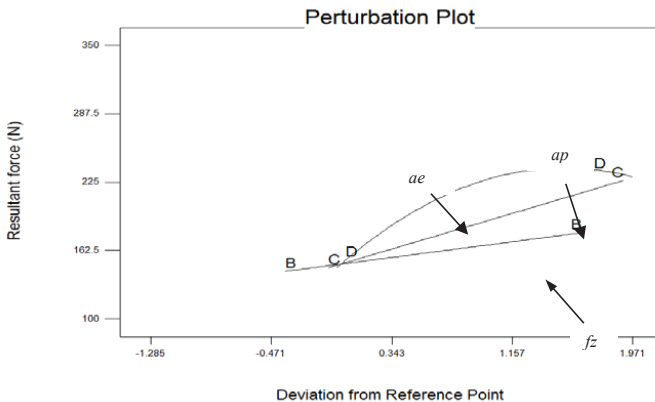

Figure 3. Perturbation plot of optimized cutting parameters.

3.0   CONCLUSIONS

This paper shows the relationship between cutting parameter and cutting force during end milling. A mathematical model based on RSM method has successfully been developed to calculate the resultant force. The prediction for resultant force largely agrees with the 29 series of experimental result. This study shows the cutting force can be significantly reduced by controlling width of cut. Width of cut, ae of 0.2 mm is suggested to minimize cutting force generated. The experiment shows the ball nose application able to reduce cutting force as low as 150 N.

ACKNOWLEDGEMENTS

REFERENCES

Alauddin, M., El Baradie, M. A., & Hashmi, M. S. J. (1996). Modelling of cutting force in end milling Inconel 718. *Journal of Materials Processing Technology*, 58(1), 100-108.

Alauddin, M., Mazid, M. A., El Baradi, M. A., & Hashmi, M. S. J. (1998). Cutting forces in the end milling of Inconel 718. *Journal of Materials Processing Technology*, 77(1-3), 153-159.

Alloys, N. S. (2011). 718 Inconel® Nickel Alloy Bar. Retrieved 3 March, 2011, from http://www.nsalloys.com/718-nickel-alloy-bar.html

Ezugwu, E. O., Wang, Z. M., & Machado, A. R. (1999). The machinability of nickel-based alloys: a review. *Journal of Materials Processing Technology*, 86(1-3), 1-16.

Izamshah, R., Mo, J. P. T., & Ding, S. (2012). Hybrid deflection prediction on machining thin-wall monolithic aerospace components. *Journal of Engineering Manufacture*, 226(4), 592-605.

Kalluri, S., & Halford, G. R. (1995). Fatigue Behavior and Deformation Mechanisms in Inconel 718 Superalloy Investigated. Retrieved from http://www.grc.nasa.gov/www/rt/rt1995/5000/5220k.htm

Kitagawa, T., Kubo, A., & Maekawa, K. (1997). Temperature and wear of cutting tools in high-speed machining of Inconel 718 and Ti6Al6V2Sn. *Wear*, 202(2), 142-148.

Liao, Y. S., Lin, H. M., & Wang, J. H. (2008). Behaviors of end milling Inconel 718 superalloy by cemented carbide tools. *Journal of Materials Processing Technology,* 201(1-3), 460-465.

Montgomery, D. C. (2009). Design and Analysis of Experiments (7th ed.). Hoboken: John Wiley & Sons, Inc.

Sharman, A., Dewes, R. C., & Aspinwall, D. K. (2001). Tool life when high speed ball nose end milling Inconel 718. *Journal of Materials Processing Technology,* 118(1-3), 29-35.

Ulutan, D., & Ozel, T. (2011). Machining induced surface integrity in titanium and nickel alloys: A review. *International Journal of Machine Tools & Manufacture,* 51, 31.